Simplification of Full Homogenized Macro-Scale Model for Lithium-ion Batteries

Salman Qadir[a,1,*], Guang Li[a], Zheng Chen[a]

[a] *School of Engineering and Materials Science, Queen Mary University of London, London, E1 4NS, United Kingdom*

Abstract

A simplified model based on the novel full homogenized macro-scale model (FHM) is proposed to reduce the computational time of the FHM model with trivial loss of fidelity. The simplified FHM model is compared with a simplified model based on the pseudo-two-dimensional (P2D) model. The FHM model is based on the homogenization theory, while the volume averaging technique is the basis of the P2D model. Diffusion Partial differential equations (PDEs) are approximated by ordinary differential equations with time-varying coefficients. The intercalation current and conduction equation are also approximated to develop variants of the simplified model. The diffusion and reaction rate parameters of the FHM model are more accurate at high temperatures than the parameters based on the empirical Bruggeman method, as the FHM model parameters are based on the numerical model of the electrode structure. The simulations results verify that, compared with a similar simplified model based on the P2D model, the proposed simplified FHM model is more accurate at 318K and higher temperature. The output voltage predicted by the proposed simplified model and the simplified P2D model has a root mean square (RMS) tracking error of 0.6% and 2%, respectively, at 1C input current and 318K temperature. The computational time of the proposed simplified model is reduced by 35% compared with that of the FHM model, highlighting its superior performance. Discretization of the model is accomplished using orthogonal collocation.

Keywords: Pseudo-Two Dimensional (P2D); Full Homogenized Macro-Scale (FHM); Reduced Order Model (ROM); Doyle Fuller Newman (DFN); Battery Management System (BMS).

1. Nomenclature

* Corresponding author
Email addresses: salman.qadir@qmul.ac.uk (Salman Qadir), g.li@qmul.ac.uk (Guang Li), chen@kust.edu.cn (Zheng Chen)
URL: https://www.sems.qmul.ac.uk/research/groups/controlsystems/ (Guang Li)

a	Electrode specific surface area,[1/m]	A_{cell}	Electrode cross-sectional area $[m^2]$
C_e	Li-ion concentration in the electrolyte, $[mol/m^3]$	$\bar{c}$	Average Li-ion concentration in the electrode, $[mol/m^3]$
C_s	Li-ion concentration in the electrode, $[mol/m^3]$	$C_{j,m}$	Maximum Li-ion concentration in solid, $[mol/m^3]$
C_{sc}	Li-ion concentration at the surface of electrode, $[mol/m^3]$	$\bar{c}_e$	Average concentration in electrolyte, $[mol/m^3]$
D_e	Electrolyte diffusion constant, $[m^2/s]$	D_s	Electrode diffusion constant, $[m^2/s]$
F	Faraday's constant, $[Vs\Omega^{-1}mol^{-1}]$	I_{app}	Applied current, [A]
J	Interaction current, $[A/m^3]$	K_e	Electrolyte conductivity, $[S^{-1}M^{-1}]$
k_j	P2D electrochemical reaction-rate constant, $Am^{2.5}mol^{-1.5}$	k_j^*	FHM electrochemical reaction rate constant, $Amol^{-1}$
K_s	Electrode conductivity, $[S^{-1}M^{-1}]$	r	Radial coordinate [m]
R	Universal gas constant, $[J\cdot mol^{-1}\cdot K^{-1}]$	R_c	Collector resistance, [Ω]
R_s	Radius of active particle, $[m]$	t	Time, $[s]$
t_+	Transference number	T	Temperature,$[K]$
U	Electrode open circuit potential, $[V]$	$\bar{q}$	Average flux in electrode.$[mol/m^4]$
θ	Normalized concentration in electrode	ϕ_s	Electrode potential, V
ϕ_e	Electrolyte potential, V		defined as the ratio of ℓ and L
η	Over potential, V	η_e	Electrolyte volume fraction

Table 1: List of symbols

2. Introduction

2.1. Literature Review

To optimize the battery efficiency, Battery Management System (BMS) plays a vital role in ensuring the battery's safe operation in various conditions. BMS monitors essential state variables of the cell such as state of charge (SoC), state of health (SoH), and temperature, among others to avoid misuse of the battery [1] [2].

The mathematical model of a Li-ion cell is an essential part of BMS to estimate the state variables. Over the past decades, various mathematical models have been developed with a range of computational complexity and accuracy such as equivalent circuit models, data driven models, electrochemical models [3], [4], [5]. Equivalent circuit models are simple and computationally most efficient as compared to other models. Equivalent circuit models are composed of electric circuit elements such as voltage sources, resistors, and capacitors. These fictitious elements are added to obtain a current-voltage characteristic curve approximately equivalent to a Li-ion cell's experimental current-voltage characteristic curve. The battery states such as SoC and SoH calculated using the equivalent circuit models are less accurate as compared to the computationally intensive electrochemical models [6], [7].

Recently attempts have been made to improve SoC estimation using either advanced equivalent circuit models or adaptive neuro-fuzzy inference systems (ANFIS) based models. However the proposed models are either not accurate or health-conscious enough as compared to electrochemical models [8], [9], [10], [11]. L. Ma *et al.* has proposed joint SoC estimation based on a long short-term memory neural network. The approach shows better results as compared to other machine learning algorithms but is not accurate enough as compared to the proposed approach [12]. H Yang *et al.* and H F Khan *et al.* have proposed SoC estimation based on variants of the Kalman filter. However, the model used is a basic equivalent circuit model. The performance can be improved further by using accurate models [13],[14].

Electrochemical models are derived from the first principles of the cell, such as the Doyle Fuller Newman (DFN) model. Electrochemical models precisely describe the internal dynamics of the cell, such as diffusion, conduction, and intercalation. Electrochemical models are more reliable than equivalent circuit models due to their high accuracy. However, using an electrochemical model such as the DFN model for real-time processing is not feasible due to the high computational load. DFN model is mainly used as a reference to evaluate the accuracy of other simplified models. A reduced electrochemical model such as a single-particle model is imperative for real-time processing [15], [16].

Diffusion and conduction parameters of the DFN model are key parameters that influence the fidelity of the DFN model. The empirical Bruggeman method is used to obtain the parameters. The method leads to inaccurate results in certain conditions [17]. Recently a more accurate model called the full homogenized macro-scale (FHM) model is developed. FHM model inculcates the structural composition of the electrode and calculates the value of dif-

fusion and conduction parameters D_e, D_s, K_e and K_s by developing a numerical model of electrode architecture. The model is more accurate for estimation in conditions such as low values of SoC, a high value of temperature, and a C-rate. However performance of both models is similar at room temperature [18], [19],[20]. The FHM model is computationally intensive and suitable for offline estimation and analysis.

We have used a one-dimensional FHM and DFN model in this article. A 'pseudo' spherical dimension r is included in the DFN model to describe the diffusion of Li-ions within electrode particles. The model is also known as the pseudo-two-dimensional (P2D) Model [21]. The FHM model is computationally less intensive than the P2D model as it has only one dimension.

2.2. Novelty

As the P2D model fails to predict the output voltage of the cell accurately at high temperatures , i.e. above 318K and low value of charge [22]. The performance of P2D based simplified models deteriorates further at a high value of input current due to approximation.

The purpose of this article is to present a simplified model based on the FHM model, which is computationally less intensive than the FHM model but more accurate as compared to the simplified P2D model at high temperature. We expect the simplified FHM model to show performance similar to the FHM model up to a 4C input current, which enables us to develop an accurate model fast enough to be implementable in real-time.

The idea of the proposed model is similar to the simplified models developed by Subramanian *et al.* [23], Han *et al.* [24] and Deng *et al.* [25]. The articles, as mentioned earlier, are based on the idea that ordinary differential equations with time-varying coefficients can approximate the Li-ion concentration. Replacement of the spatial double derivative with time-varying coefficients simplifies the models and facilitates fast implementation.

Although some researchers have recommended high order polynomials [23], we prefer the second-order polynomial to approximate the Li-ion concentration in electrode and electrolyte. Recently it has been observed that the approximate electrode models developed using higher-order polynomials introduce unwanted characteristics such as eigenvalues with positive real parts, non-minimum phase zeros. In contrast, the actual electrode model does not exhibit these characteristics. However, Second-order polynomials provide smaller bandwidth and less precision in transients as compared to higher-order polynomial approximations [26]. Another feature of polyno-

mials is time variance.The coefficients of polynomials are calculated at every iteration.

The rest of the article is organized as follows. First, We present the FHM model and the P2D model, followed by the simplified FHM model, the simplified P2D model and further simplification. Next we offer a discussion on results and conclusions. Table of parameter values used for the simulation are provided in the Appendix.

3. Modelling

3.1. Pseudo Two Dimensional (P2D) Model

The electrodes in the cell consist of multiple spherical particles. The P2D electrode diffusion dynamics for a single particle is described by the equation (1). The variable r defines the radial dimension. The Li-ion exchange between electrode and electrolyte, known as intercalation current, occurs at the particle's surface. The boundary conditions at the center and surface of spherical particles are mentioned as follows.

$$\frac{\partial c_{s,j}}{\partial r}\Big|_{r=0} = 0, \quad \frac{\partial c_{s,j}}{\partial r}\Big|_{r=R_s} = -\frac{J_j}{F \cdot a_j} = \frac{-J_j \cdot R_{s,j}}{D_{s,j} \cdot F \cdot 3\eta_j} \tag{6}$$

The net Li-ion diffusion at the center of the particle is zero. The Li-ion diffusion at the surface is equivalent to the intercalation current scaled by the Faraday's constant F and the electrode interfacial surface area a_s to account for the porosity of the electrode. $R_{s,j}$, c_s and $D_{s,j}$ are the radius of the sphere, solid concentration and solid diffusion parameter respectively. Initial concentration is given by the initial stoichiometry variable $\theta_{j,init}$, i.e. normalized value of concentration. Suffix j denotes negative and positive electrodes.

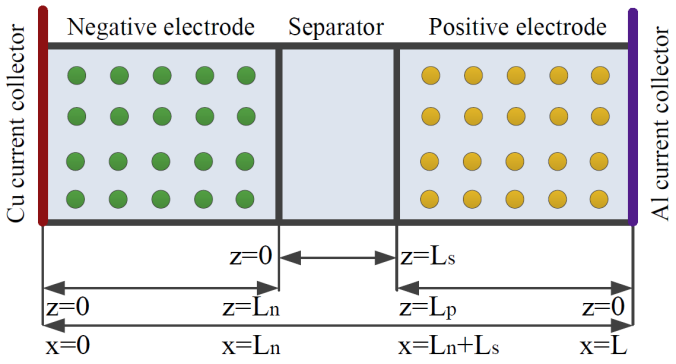

Figure 1: Li-ion cell schematic [27].

Table 2: Comparison of P2D and FHM mathematical models [17]

Eq. No	FHM Model	P2D Model	Part
(1)	$\frac{\partial c_{s,j}(x,t)}{\partial t} = D_{s,j}\frac{\partial^2 c_{s,j}(x,t)}{\partial x^2} - \frac{J_j(x,t)}{F}$	$\frac{\partial c_{s,j}(x,r,t)}{\partial t} = \frac{1}{r^2}\frac{\partial}{\partial r}\left(D_{s,j} r^2 \frac{\partial c_{s,j}(x,r,t)}{\partial r}\right)$	Electrode Diffusion
(2)	$\eta_{e,j}\frac{\partial c_{e,j}(x,t)}{\partial t} = \frac{J_j(x,t)}{F} + D_{e,j}\frac{\partial^2 c_{e,j}}{\partial x^2} + \frac{RTt_+^2}{F^2}K_{e,j}\frac{\partial^2 ln\ c_{e,j}}{\partial x^2} + \frac{t_+}{F}K_{e,j}\frac{\partial^2 \phi_{e,j}}{\partial x^2}$	$\eta_{e,j}\frac{\partial c_{e,j}(x,t)}{\partial t} = \frac{\partial}{\partial x}\left(D_{e,j}\frac{\partial c_{e,j}}{\partial x}\right) + \frac{(1-t_+)J_j(x,t)}{F}$	Electrolyte Diffusion
(3)	$K_{s,j}\frac{\partial^2 \phi_s(x,t)}{\partial x^2} = J_j(x,t)$	$K_{s,j}\frac{\partial^2 \phi_s(x,t)}{\partial x^2} = J_j(x,t)$	Electrode Potential
(4)	$\frac{RTt_+}{F}K_{e,j}\frac{\partial^2 lnc_e}{\partial x^2} + K_{e,j}\frac{\partial^2 \phi_e(x,t)}{\partial x^2} = -J_j(x,t)$	$\frac{2RT(1-t_+)}{F}K_{e,j}\frac{\partial^2 lnc_e}{\partial x^2} + K_{e,j}\frac{\partial^2 \phi_e(x,t)}{\partial x^2} = -J_j(x,t)$	Electrolyte Potential
(5)	$\eta = \phi_s(x) - \phi_e(x) - U(\theta)$ $i_0 = ((c_e c_s)(1 - \frac{c_{j,s}}{c_{j,m}}))^{0.5}$ $J_j(x,t) = i_0 2k_j sinh\left(\frac{F\eta_j}{2RT}\right)$	$\eta = \phi_s(x) - \phi_e(x) - U(\theta)$ $i_0 = ((c_e c_{j,s})(c_{j,m} - c_{j,s}))^{0.5}$ $J_j(x,t) = i_0 2k_j \cdot sinh\left(\frac{F\eta_j}{2RT}\right)$	Intercalation Current

The Li-ion diffusion inside the electrolyte is described by the equation (2). Initial, boundary and continuity conditions are mentioned in the equations (10) and (13) respectively.

c_e, $\eta_{e,j}$ and x are the liquid phase (electrolyte) concentration, electrolyte volume fraction and physical dimension variable. L, L_n, L_s and L_p are the length of the cell, anode, separator and cathode, respectively. D_e is the electrolyte diffusion parameter. The initial value of the electrolyte concentration is constant and mentioned in the Appendix. There is no Li-ion flow between the electrode and the current collector. The electrolyte medium exists in a continuum throughout the cell. The concentration and the flux are assumed to be equal at both sides of the electrode-separator interface.

Equation (5) describes the intercalation current J_j, whereas the open circuit potential is given as follows.

$$U_p(\theta) = -10.72\theta^4 + 23.88\theta^3 - 16.77\theta^2 + 2.595\theta + 4.563 \tag{7}$$

$$U_n(\theta) = 0.1493 + 0.8493\exp(-61.79\theta) + 0.3824\exp(-665.8\theta) - 1\exp(39.42\theta - 41.92) \\ -0.03131\arctan(25.59\theta - 4.099) - 0.009434\arctan(32.49\theta - 15.74) \tag{8}$$

η is the over-potential and denotes the potential difference required for the Li-ion exchange between electrode and electrolyte. ϕ_s, ϕ_e and U are the electrode potential, electrolyte potential and open circuit potential respectively [28]. θ, $c_{j,m}$, k_j, T and R are the normalised solid concentration, maximum solid concentration, reaction rate parameter, temperature, and universal gas constant respectively.

The dynamics of the solid phase potential drop ϕ_s and liquid phase potential drop ϕ_e is given by the equations (4) and (3) respectively. $K_{s,j}$ and $K_{e,j}$ are the conductivity parameters for solid and liquid, respectively. Initial conditions and boundary conditions of electrode and electrolyte are described by the equations (11) and (12) respectively, whereas continuity conditions of the electrolyte potential are described by the equation (14). The initial value of the potential drop in the electrolyte is assumed zero, whereas the potential drop across the electrode is equal to the open circuit potential difference. The solid potential at the anode collector is the reference. The value of potential drop in the electrolyte at the electrode-collector interface is zero.

3.2. Full Homogenised Macro-scale (FHM) Model

The FHM model consists of two partial differential equations (PDEs) and three algebraic equations as mentioned in Table 2, while initial and boundary conditions are mentioned in Table 3. The Li-ion diffusion in the solid phase (electrode) is governed by Fick's law as mentioned in equation (1). The boundary conditions are mentioned as follows.

$$\left.\frac{\partial c_{s,j}}{\partial x}\right|_{x=0,L} = 0, \quad \left.\frac{\partial c_{s,j}}{\partial x}\right|_{x=L_n, L_n+L_s} = -\frac{J_j \cdot L_j}{D_{s,j} \cdot F \cdot 3\eta_j} \tag{15}$$

The Li-ion diffusion at the collector end of the electrode is zero. The Li-ion diffusion at the separator end is equivalent to the scaled intercalation current. The diffusion equation of the FHM model includes the intercalation current, whereas the intercalation current only appears in the boundary condition of the P2D model solid diffusion equation. The boundary condition at the electrode-separator interface is the same as the corresponding P2D model boundary condition. The variable $R_{s,j}$ in the earlier mentioned boundary condition is replaced by L_j. The

Table 3: Initial and Boundary conditions common to P2D model and FHM model [17]

Equation Number	Initial conditions	Boundary conditions	Part
(9)	$c_{s,n} = \theta_{n,init} \cdot c_{s,n,m}$ $c_{s,p} = \theta_{p,init} \cdot c_{s,p,m}$	-	Electrode Diffusion
(10)	$c_{e,n} = c_{e,sep} = c_{e,p} = c_{e,a}$	$\frac{\partial c_{e,j}}{\partial x}\big\|_{x=0,L} = 0$	Electrolyte Diffusion
(11)	$\phi_{s,n} = 0$ $\phi_{s,p} = U_{p,init} - U_{n,init}$	$\phi_{s,n}\big\|_{x=0} = 0$ $\frac{\partial \phi_{s,p}}{\partial x}\big\|_{x=L} = -\frac{I_{app}}{A_{cell} \cdot K_{s,p}}$	Electrode Potential
(12)	$\phi_{e,n} = \phi_{e,sep} = \phi_{e,p} = 0$	$\frac{\partial \phi_{e,j}}{\partial x}\Big\|_{x=0,L} = 0$	Electrolyte Potential
(13)	–	$\frac{\partial c_{e,j}}{\partial x}\big\|_{x=L_{n-}} = \frac{\partial c_{e,j}}{\partial x}\big\|_{x=L_{n+}}$ $c_{e,j}\big\|_{x=L_{n-}} = c_{e,j}\big\|_{x=L_{n+}}$ $\frac{\partial c_{e,j}}{\partial x}\big\|_{x=L_n+L_{s-}} = \frac{\partial c_{e,j}}{\partial x}\big\|_{x=L_n+L_{s+}}$ $c_{e,j}\big\|_{x=L_n+L_{s-}} = c_{e,j}\big\|_{x=L_n+L_{s+}}$	Electrolyte Diffusion Continuity Equation
(14)	–	$\frac{\partial \phi_{e,j}}{\partial x}\big\|_{x=L_{n-}} = \frac{\partial \phi_{e,j}}{\partial x}\big\|_{x=L_{n+}}$ $\phi_{e,j}\big\|_{x=L_{n-}} = \phi_{e,j}\big\|_{x=L_{n+}}$ $\frac{\partial \phi_{e,j}}{\partial x}\big\|_{x=L_n+L_{s-}} = \frac{\partial \phi_{e,j}}{\partial x}\big\|_{x=L_n+L_{s+}}$ $\phi_{e,j}\big\|_{x=L_n+L_{s-}} = \phi_{e,j}\big\|_{x=L_n+L_{s+}}$	Electrolyte Potential Continuity Equation

remaining equations of the FHM model are similar to the P2D model.

4. Model Simplification

4.1. Simplified P2D Electrode Diffusion Model

The simplified electrode diffusion model presented by Subramanian [23] is used in present work. The following equations describe the approximate solid concentration.

$$\frac{d\bar{c}(t)}{dt} = -3\frac{J_j}{a_s \cdot F \cdot R_s} \tag{16}$$

$$\frac{D_s}{R_s}[c_{sc}(t) - \bar{c}(t)] = \frac{-J_j}{5a_s \cdot F} \tag{17}$$

The variables $\bar{c}(t)$ and c_{sc} are the average solid concentration and the surface concentration respectively. Since the open circuit potential and other variables are function of the surface concentration c_{sc} and state of charge (SoC) is a function of average concentration $\bar{c}(t)$, (16) and (17) are used for simulating the electrode diffusion model.

4.2. Simplified FHM Electrode Diffusion Model

We propose that the solid phase concentration along the whole length of an electrode can be approximated by a second order polynomial as shown below.

$$c_s(x,t) = a(t) + b(t)\Big(\frac{x^2}{L_j^2}\Big) \tag{18}$$

We put the value of c_s from the equation (18) in the equation (15) and get the following equation.

$$2\frac{D_s b(t)}{L_j} = \frac{-J(L_j) \cdot L_j}{3\eta_s \cdot F} \tag{19}$$

The coefficient $b(t)$ can be calculated from the equation (19). Another equation is required to find value of $a(t)$. Following procedure is adopted to solve this problem. The average concentration $\bar{c}(t)$ is related to the solid phase concentration as follows.

$$\bar{c}(t) = \frac{1}{L_j}\int_{x=0}^{L_j} c(x,t)dx \tag{20}$$

$$\bar{c}(t) = a(t) + \frac{b(t)}{3} \tag{21}$$

Averaging both sides of the equation (1) gives us the following equation to calculate the average concentration $\bar{c}(t)$.

$$\frac{1}{L_j}\int_{x=0}^{L_j}\Big[\frac{\partial c_s}{\partial t} - D_s\frac{\partial^2 c_s}{\partial x^2} + \frac{J(x,t)}{F}\Big]dx = 0 \tag{22}$$

$$\frac{d\bar{c}(t)}{dt} = -\frac{J(L_j)}{3\eta_s \cdot F} - \frac{I_{app}}{F \cdot L_j} \tag{23}$$

$$I_{app} = \frac{I}{A} \tag{24}$$

A is the surface area of cell collector. I is the input current. Average concentration $\bar{c}(t)$ is calculated using the equation (23). The value of unknown time varying coefficients are calculated using the equations (19) and (21). The solid phase concentration is calculated using the equation (18). Step-wise algorithm is presented in the table 4.

Table 4: Algorithm for simplified FHM electrode diffusion model.

Step No	Step
1	Available data : Initial discrete time k=0, Initial average Li-ion concentration in electrode $\bar{c}(k)$ based on initial SoC.
2	Calculate $\bar{c}(k)$ using the equation (23)
3	Calculate $b(t)$ using the equation (19).
4	Calculate $a(t)$ using the equation (21).
5	Calculate solid phase concentration $c_s(t)$ using the equation (18)..
6	Update the value of time k and initial condition $\bar{c}(k)$ for next iteration.
7	Repeat step 2 to step 6 for next sampling instant.

4.3. Simplified Electrolyte Diffusion Model

Electrolyte diffusion equation (2) of FHM model is simplified by using (4).

$$\eta_{e,j}\frac{\partial c_{e,j}(x,t)}{\partial t} = \frac{(1-t_+)J_j(x,t)}{F} + D_{e,j}\frac{\partial^2 c_{e,j}}{\partial x^2} \tag{25}$$

FHM electrolyte diffusion equation (25) is similar to the P2D electrolyte diffusion equation. The method in [24] and [25] is used to simplify FHM liquid phase (electrolyte) diffusion equation. The physical dimension variable x

is replaced with variable z to simplify the derivation. Li-ion concentration in the three regions, i.e. anode, separator and cathode, is approximated by a second-order polynomial as given below.

$$c_{e,n}(z) = a_1 z^2 + a_0, \quad 0 \le z \le L_n \tag{26}$$

$$c_{e,s}(z) = a_4 z^2 + a_3 z + a_2, \quad 0 \le z \le L_s \tag{27}$$

$$c_{e,p}(z) = a_6 z^2 + a_5, \quad 0 \le z \le L_p \tag{28}$$

The first order terms in the equations (26) and (28) are zero due to boundary condition mentioned in the equation (12). Following four equations are derived by putting the value of $c_{e,j}(z)$ in continuity conditions given by the equation (13).

$$a_1 L_n^2 + a_0 = a_2 \tag{29}$$

$$a_6 L_p^2 + a_5 = a_4 L_s^2 + a_3 L_s + a_2 \tag{30}$$

$$2a_1 L_n D_{e,n} = a_3 D_{e,s}^{eff} \tag{31}$$

$$-2a_6 L_p D_{e,p} = (2a_4 L_s + a_3) D_{e,s} \tag{32}$$

Total amount of Li-ions in the anode, separator and cathode $Q_{e,j}$ is calculated by integrating the equations (26), (27) and (28) respectively.

$$Q_{e,n}(t) = \eta_{e,n} \int_0^{L_n} c_{e,n}(z)\,dz = \eta_{e,n}\left(\frac{a_1 L_n^3}{3} + a_0 L_n\right) \tag{33}$$

$$Q_{e,s}(t) = \eta_{e,s} \int_0^{L_s} c_{e,s}(z)\,dz = \eta_{e,s}\left(\frac{a_4 L_s^3}{3} + \frac{a_3 L_s^2}{2} + a_2 L_s\right) \tag{34}$$

$$Q_{e,p}(t) = \eta_{e,p} \int_0^{L_p} c_{e,p}(z)\,dz = \eta_{e,p}\left(\frac{a_6 L_p^3}{3} + a_5 L_p\right) \tag{35}$$

We calculate derivatives of $Q_{e,j}$ subject to electrolyte boundary and continuity conditions to obtain the following equations.

$$\begin{aligned} \frac{d}{dt}Q_{e,n}(t) &= \frac{I_{app}(1-t_+)}{F} + D_{e,n}\frac{\partial c_{e,n}}{\partial z}\bigg|_{z=0}^{z=L_n} \\ \frac{d}{dt}Q_{e,n}(t) &= \frac{I_{app}(1-t_+)}{F} + D_{e,n} 2a_1 L_n \end{aligned} \tag{36}$$

$$\begin{aligned} \frac{d}{dt}Q_{e,p}(t) &= \frac{I_{app}(1-t_+)}{F} + D_{e,p}\frac{\partial c_{e,p}}{\partial z}\bigg|_{z=0}^{z=L_p} \\ \frac{d}{dt}Q_{e,p}(t) &= -\frac{I_{app}(1-t_+)}{F} + D_{e,p} 2a_6 L_p \end{aligned} \tag{37}$$

$$\frac{d}{dt}Q_{e,s}(t) = D_{e,s}\frac{\partial c_{e,s}}{\partial z}\Big|_{z=0}^{z=L_s}$$
$$\frac{d}{dt}Q_{e,s}(t) = D_{e,s}2a_4L_s \tag{38}$$

The seven unknown coefficients are solved using the seven equations, i.e. (29), (30), (31), (32), (36), (37) and (38). The equations (26),(27) and (28) are used to simulate the electrolyte diffusion model. Step-wise algorithm is provided in table 5

Table 5: Algorithm for the Simplified electrolyte Diffusion Model [24], [25] .

Step No	Step
1	Available Data:Initial discrete time k=0, Initial total concentration of Li-ion in electrolyte $\bar{Q_{e,j}}(0)$ based on initial concentration.
2	Calculate $a_0, a_1 ... a_6$ using the equations (29), (30), (31), (32), (36), (37) and (38) .
3	Calculate total Li-ion concentration $Q_{e,j}(k)$ at next time instant using the equations (26),(27) and (28).
4	Update the value of time k and initial condition $Q_{e,j}(k)$ for the next iteration.
5	Repeat step 2 to step 6 for next sampling instant.

4.4. Approximation of Intercalation Current

The intercalation current J_j is assumed constant. The following equations are derived by manipulating the equation (4).

$$J_n = \frac{I_{app}}{L_n \cdot F}$$
$$J_p = \frac{-I_{app}}{L_p \cdot F} \tag{39}$$

This model is called Further simplified FHM model.

4.5. Simplification of Algebraic Equations

Approximation for the algebraic equation of Li-ion cell is based on the work of S. J. Moura [29]. The intercalation current J_j is assumed constant. Exchange current density $i_0(x,t)$ is approximated by the spatial average value

$\bar{i_o}(t)$ and approximate over-potential $\bar{\eta}$ is given by the following equation.

$$\bar{\eta}(t) = \frac{RT}{\alpha F} sinh^{-1}\Big(\frac{I_{app}}{2\alpha L\bar{i_0}(t)}\Big) \tag{40}$$

$$V = \phi_{s,p}(L) - \phi_{s,n}(0) \tag{41}$$

$$\phi_s(x,t) = \bar{\eta} + \phi_e(x,t) + U(x,t) \tag{42}$$

The procedure mentioned in ref. [29] is used to simplify the output voltage and potential equation. Simplified output voltage equation is mentioned as follows.

$$\begin{aligned} V = \bar{\eta_p}(t) - \bar{\eta_n}(t) + U_p(\theta(L)) - U_n(\theta(L)) + \\ k_1 I_{app} + k_2(\ln(c_e(L)) - \ln(c_e(0))) \end{aligned} \tag{43}$$

$$k_1 = \frac{L_n + 2L_s + L_p}{2K_{eff}} \tag{44}$$

$$k_2 = \frac{2RT(1-t_+)K_{eff}}{F} \tag{45}$$

We label this model as SFHM 2 model.

5. Orthogonal Collocation

5.1. Spatial Discretisation

Spatial discretisation is done using orthogonal collocation developed by Adrien [21] . The solution $u(x,t)$ of a PDE is described by the following equation.

$$u_N(x,t) = \sum_{j=0}^{N} \hat{u}_j(t)\phi_j(x), \qquad x\epsilon[-1,1] \tag{46}$$

$$\phi_j(x) = \frac{(-1)^{j+1}(1-x^2)T_N^r(x)}{\bar{c}_j N^2(x-x_j)}, \qquad x\epsilon[-1,1] \tag{47}$$

$\bar{c}_j = 0$ for $j = 0, N$ and $\bar{c}_j = 1$ otherwise $T_N(x)$ denotes the Chebyshev polynomial of degree N. $\hat{u}_j(t)$ is equal to the value of solution $u(x_j,t)$ at discretised nodes known as collocation points. The collocation points are given by the following equation.

$$x_i = cos\Big(\frac{\pi i}{N}\Big), \qquad i = 0, 1..N. \tag{48}$$

The p^{th} derivative of $u(x,t)$ at collocation points is calculated as follows.

$$u_N^p(x_i) = \sum_{j=0}^{N} d_{i,j}^p u_N(x_j) \tag{49}$$

$d_{i,j}^p$ is calculated by finding the derivative of the function $\phi_j(x)$. Chebyshev polynomials are are computed offline and stored to reduce the computational burden. The derivative equation is written in matrix form as follows.

$$\mathbf{u}^p = D_N^p \mathbf{u} \tag{50}$$

Similarly integration or quadrature of $u(x,t)$ is calculated as follows.

$$u_N^p(x_i) = \sum_{j=0}^{N} \alpha_{i,j} u_N(x_j) \tag{51}$$

$\alpha_{i,j}$ is calculated by finding the integration or quadrature of the function $\phi_j(x)$. MATLAB ®functions for the differentiation matrix, integration matrix etc. provided by [30] and [20] are used in this work. Consider the discretised potential equation in electrode and electrolyte as an example. The equations are written in matrix form as shown next.

$$K_{s,j}[D_N^2]_{NxN}[\phi_s]_{(N+1)x1} = [J]_{Nx1} \tag{52}$$

$$\frac{RTt_+}{F} K_{e,j}[D_N^2]_{NxN}[ln(c_e)]_{(N+1)x1} + K_{e,j}[D_N^2]_{NxN}[\phi_e(z,t)]_{(N+1)x1} = [-J_j]_{Nx1} \tag{53}$$

We have N equations but $N+2$ variables. We use the boundary conditions to solve the two additional variables. To enforce boundary conditions the first and last rows of the differentiation matrix are used. Consider the following example.

$$\frac{\partial \phi_{e,j}}{\partial x}\Big|_{z=0,L} = 0 \tag{54}$$

The boundary conditions are solved to get the values of two unknown variables.

5.2. Temporal Discretisation

Equations (23),(36), (37) and (38) are dynamic equations of the simplified model and represented as follows.

$$\dot{x}(t) = g(x(t), u(t)) \tag{55}$$

Output equation is represented as follows.

$$y = h(x,u) \tag{56}$$

g, x, u, y and h are state function, system states, input current,output variable, and output function respectively. Solid and liquid concentration variables are considered the state variables of the cell. Current is considered as the input. Cell voltage and SoC are considered output. SoC of either electrode is calculated by the following equation.

$$SoC_j(t) = \frac{\theta_j^{avg}(t) - \theta_j^{0\%}}{\theta_j^{100\%} - \theta_j^{0\%}} \tag{57}$$

The normalized average concentration for P2D model and FHM model are calculated respectively by the following equation.

$$\theta_j^{avg}(t) = \frac{3}{L_j R_{s,j}^3} \int_0^{L_j} \int_0^{R_{s,j}} r^2 \frac{c_{s,j}(x,r,t)}{c_{j,m}} dr dx \tag{58}$$

$$\theta_j^{avg}(t) = \frac{1}{L_j} \int_0^{L_j} \frac{c_{s,j}(x,t)}{c_{j,m}} dx \tag{59}$$

$\theta_j^{0\%}$ and $\theta_j^{100\%}$ denote 0% and 100% SoC respectively and mentioned in the appendix.

The equation is discretised using orthogonal collocation. The details of orthogonal collocation are discussed in section 5. The n dimensional matrix equation corresponding to n collocation points is expressed as follows.

$$X_{N\times 1} = X(t_0)_{N\times 1} + \frac{t_f - t_0}{2} A_{N\times N} G_{N\times 1}(X,U) \tag{60}$$

$A_{N\times N}$ is the pseudos-spectral integration matrix. t_0 and t_f are the initial and final times respectively. Value of state matrix G is given as follows.

$$G = \begin{bmatrix} -\frac{J(L_n)}{3\eta_s \cdot F} - \frac{I_{app}}{F \cdot L_n} \\ -\frac{J(L_p)}{3\eta_s \cdot F} - \frac{I_{app}}{F \cdot L_p} \\ \frac{I_{app}(1-t_+)}{F} + D_{e,n} 2a_1 L_n \\ -\frac{I_{app}(1-t_+)}{F} + D_{e,p} 2a_6 L_p \\ D_{e,s} 2a_4 L_s \end{bmatrix} \tag{61}$$

The output equation (43) is an algebraic equation. The following equation represents the output equation in matrix form.

$$Y_{N\times 1} = H_{N\times 1}(X,U) \tag{62}$$

The value of output matrix H for voltage output is given as follows.

$$\begin{aligned} H = \bar{\eta_p}(x_j) - \bar{\eta_n}(x_j) + U_p(\theta(L)) - U_n(\theta(0)) + \\ k_1 I_{app} + k_2(\ln(c_e(L)) - \ln(c_e(0))) \end{aligned} \tag{63}$$

x_j is the collocation point or discretised time.

6. Results

Simulation results are produced using MATLAB ®.Crank-Nicolson is used for discretisation of models to produce results shown in figures 2,4,3,5 and table 6. While MATLAB ®function Ode15s and orthogonal collocation is used to produce results shown in table 7 and figure 6. Parameters are primarily obtained from [19],[20],[17],[18]. The sampling time is 1 second and the cell temperature is 318K. The percentage root mean square (RMS) error between the voltage V_i and the reference voltage $V_{ref,i}$ is calculated using the following equation to quantify the accuracy of a particular voltage signal V_i.

$$RMS\ Error = \frac{100}{mean(V_{ref})} \times \sqrt{\frac{1}{N}\sum_{i=0}^{N}(V_{ref,i} - V_i)^2} \tag{64}$$

The experimental voltage is taken as a reference for calculating RMS error. Experimental results are obtained from [18]. Consider Figure 2, We observe that at 318K, the performance of the FHM model and the proposed simplified FHM model is very good, and the value of RMS error is 0.6% for 1C current. As compared to the FHM model and the simplified FHM model, the P2D model and the simplified P2D model show relatively inaccurate performance. The value of RMS error for the P2D and the simplified P2D model is about 2% for 1C current. From Figure 2 it can be observed that the high value of RMS error for the P2D model and the simplified P2D model is mainly due to performance deterioration at low values of SoC. We also observe that the output voltage of the simplified FHM model and simplified P2D model accurately track the output of the FHM model and the P2D model respectively. Consider Figure 2, we observe that SoC estimation using the simplified P2D model is not accurate while the simplified FHM model accurately estimates SoC.

Figure 4 shows the Li-ion concentration for the FHM model and simplified FHM model in anode at various time instants. This plot is the same as the plot of the second-order polynomial, i.e. parabola $p(x) = ax^2 + bx + c$ where x represents the physical dimension of the electrode. Based on this fact, our assumption of approximating the Li-ion concentration for the FHM electrode equation using a second-order polynomial is proved correct. The same plot is observed for both electrodes at all points in time. Same observations are recorded for electrolyte, which justifies the use of quadratic polynomial for the approximation of liquid phase concentration.

The main reason for the superior performance of the FHM model and the simplified FHM model is that the FHM model is derived based on the actual structure of the electrode. In contrast, the P2D model is derived based on the

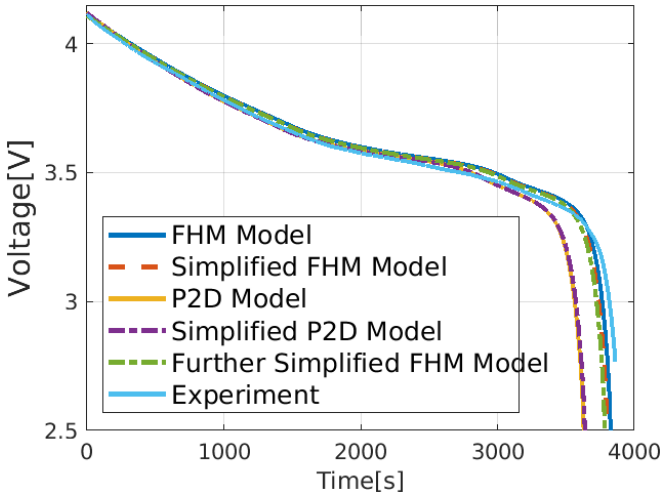

Figure 2: Output voltage of various Li-ion cell models for 1C input current at 318K temperature.

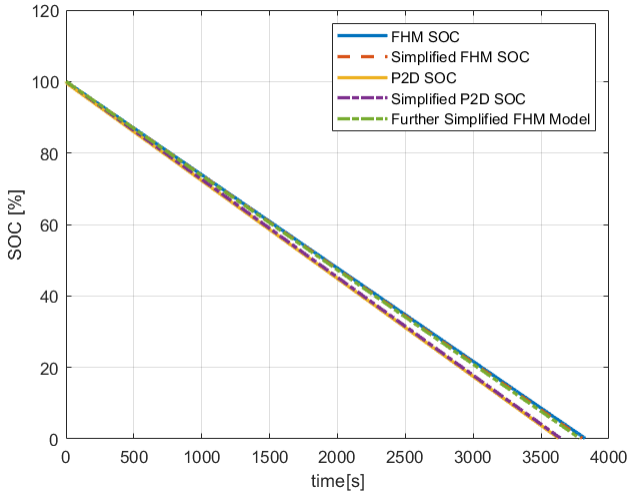

Figure 3: SoC of various Li-ion cell models for 1C input current at 318K temperature.

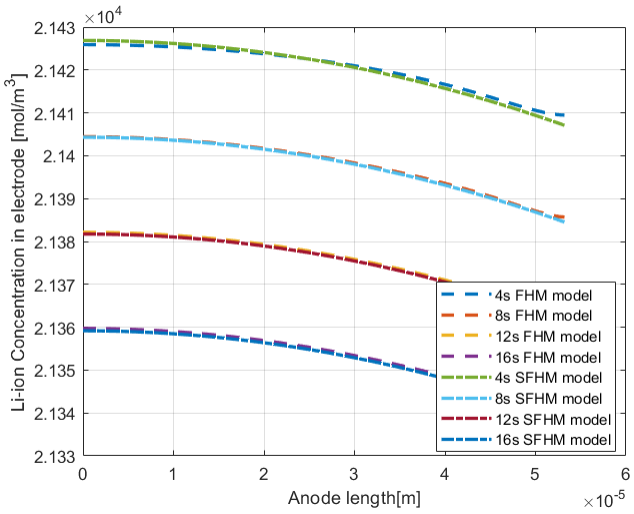

Figure 4: Li-ion concentration profile vs the length of anode for FHM model and SFHM model for 1C current input at 4,8,12 and 16s.

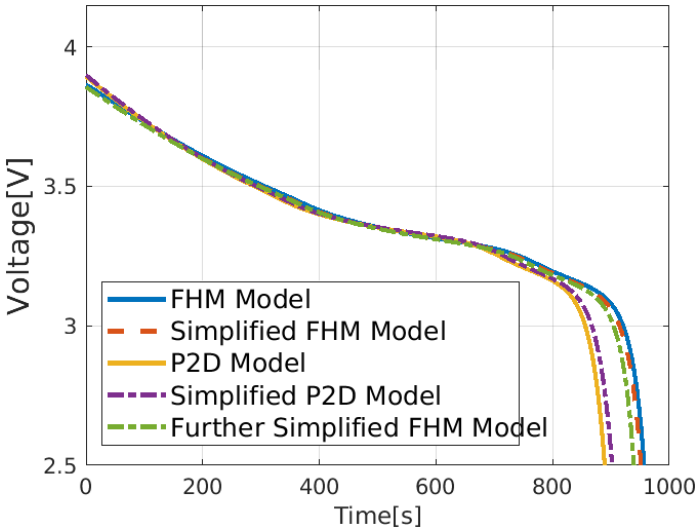

Figure 5: Output voltage of various Li-ion cell models for 4C input current at 318K temperature.

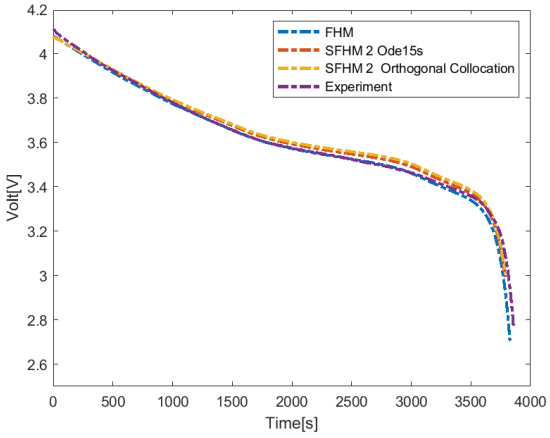

Figure 6: Comparison of output voltage for FHM model, SFHM 2 model, and experiment at 1C current input at 318K temperature.

assumption that fictitious spherical particles constitute electrode. For the FHM model, the value of temperature-dependent parameters such as the electrode diffusion parameter and the reaction rate constant is calculated based on numerical modelling of the electrode structure. The P2D model uses the empirical and relatively inaccurate Bruggeman method. We observe that the RMS error of further simplified FHM model is equal to the RMS error of the simplified FHM model for 1C current as shown in Table 6. However, if the input current is increased to 4C, the error for further simplified FHM model is increased to 3% and error for simplified FHM model is 2.1% considering FHM voltage output as reference signal The result is shown in the Figure 5.

Consider the Table 6, simulation time for FHM model is 34s, less than P2D model simulation time, i.e. 62s as FHM model has only one dimension and P2D model has additional pseudo dimension for electrode particles. The proposed simplified FHM reduced the simulation time by 35% to 20s, which is slightly less than the simplified P2D model's simulation time, i.e. 21s. Further simplification of the FHM model slightly reduces the simulation time to 19s. The proposed simplified FHM model can accurately track the output voltage of the FHM model up to 4C current with 2.1% RMS error considering FHM voltage as a reference as shown in Figure 5 and table 8.

Figure (6) compares output voltage obtained from experiment [22] with the output voltage predicted using various models i.e FHM model, SFHM 2 model, . Initial and final SoC is set to 99.9% and 0.1% respectively. The sampling time is 1 second. The cell is discharged at 1C current and 318K temperature. SFHM model is simulated using MATLAB ®Odes15s function and orthogonal collocation. Other models are simulated using the Ode15s function.

Table (7) compares the root mean square error (RMS) and simulation time per iteration between the experimen-

tal output voltage and the predicted output voltage for each model. The output voltage predicted by the SFHM 2 model using the Ode15s function and orthogonal collocation has an approximation RMS error of 1.31% and 1.28%. The models predict the output voltage with an approximation error greater than the SFHM model. The greater error is the price paid for further simplification.

Consider the simulation time of various models at 1C discharging current mentioned in Table (7). The orthogonal collocation is about 18 times faster than the ode15s function. Based on this discussion we conclude that the simplified FHM model variants combines the accurate estimation property of the FHM model and the low simulation time property of the simplified P2D model making it a good candidate for the development of BMS.

Table 6: Comparison of simulation time and RMS error for various Li-ion cell models for 1C current at 318K temperature.

Model	Simulation time	RMS Error
FHM model	$34s$	0.6%
P2D model	$62s$	2%
Simplified FHM model	$20s$	0.6%
Simplified P2D model	$21s$	2%
Further simplified FHM model	$19s$	0.6%

Table 7: Comparison of root mean square error (RMS) and simulation time for the FHM model and SFHM 2 model using various discretisation techniques at 1C current input at 318K temperature.

Model	Method	RMS Error	Simulation time (seconds)
FHM	Ode15s	0.5%	21s
SFHM 2	Ode15s	1.31%	1.5s
SFHM 2	Orthogonal collocation	1.28%	0.08s

Table 8: Comparison of voltage root mean square error (RMS) and simulation time for the FHM model, SFHM Model and SFHM 2 model considering FHM model as reference model. The input current is 4C and the temperature is 318K.

Model	Method	RMS Error	Simulation time(seconds)
SFHM	Ode15s	2.1%	1.21s
SFHM 2	Ode15s	3%	1.2s

7. Conclusion

In this study, a simplified FHM model is proposed and compared with a simplified P2D model. The simplified FHM model is developed by approximating the diffusion equations. The basic idea of approximation is that polynomial functions can accurately estimate the lithium-ion concentration at any time instant. Approximation of intercalation current and conduction equations leads to the development of variants of the simplified FHM model to trade-off accuracy with computational cost. Simulation results verify its superior performance compared to the simplified P2D model. The computational time of the proposed model is 35% less than the FHM model and close to the simplified P2D model. The simplified FHM model has a tracking RMS error of 0.6 %, while the simplified P2D model has a 2% tracking error. The model works accurately up to a current of 4C with a maximum 2.1 % error. The SFHM 2 model and orthogonal collocation further reduce the computational time to 0.08 seconds.

Observers are required for output feedback control of the cell to improve estimation in the presence of noise. Our future work will include designing observers such as moving horizon estimator, extended Kalman filter, and sliding mode observer. The model discussed in the paper is isothermal. Incorporating the thermal dynamics of the cell can improve the accuracy of the simplified FHM model .

8. Acknowledgement

This work was supported in part by the Higher Education Commission, Pakistan.

References

[1] K. Liu, K. Li, Q. Peng, C. Zhang, A brief review on key technologies in the battery management system of electric vehicles, Frontiers of Mechanical Engineering 14 (1) (2019) 47–64.

[2] M. K. Hasan, M. Mahmud, A. A. Habib, S. Motakabber, S. Islam, Review of electric vehicle energy storage and management system: Standards, issues, and challenges, Journal of Energy Storage 41 (2021) 102940.

[3] R. Xiong, J. Cao, Q. Yu, H. He, F. Sun, Critical review on the battery state of charge estimation methods for electric vehicles, Ieee Access 6 (2017) 1832–1843.

[4] J. Meng, M. Ricco, G. Luo, M. Swierczynski, D.-I. Stroe, A.-I. Stroe, R. Teodorescu, An overview and comparison of online implementable soc estimation methods for lithium-ion battery, IEEE Transactions on Industry Applications 54 (2) (2017) 1583–1591.

[5] W. Zhou, Y. Zheng, Z. Pan, Q. Lu, Review on the battery model and soc estimation method, Processes 9 (9) (2021) 1685.

[6] G. L. Plett, Extended kalman filtering for battery management systems of lipb-based hev battery packs: Part 2. modeling and identification, Journal of power sources 134 (2) (2004) 262–276.

[7] G. L. Plett, Extended kalman filtering for battery management systems of lipb-based hev battery packs: Part 3. state and parameter estimation, Journal of Power sources 134 (2) (2004) 277–292.

[8] S. Wang, C. Fernandez, C. Yu, Y. Fan, W. Cao, D.-I. Stroe, A novel charged state prediction method of the lithium ion battery packs based on the composite equivalent modeling and improved splice kalman filtering algorithm, Journal of power sources 471 (2020) 228450.

[9] M. A. Awadallah, B. Venkatesh, Accuracy improvement of soc estimation in lithium-ion batteries, Journal of Energy Storage 6 (2016) 95–104.

[10] K. V. Singh, H. O. Bansal, D. Singh, Hardware-in-the-loop implementation of anfis based adaptive soc estimation of lithium-ion battery for hybrid vehicle applications, Journal of Energy Storage 27 (2020) 101124.

[11] C. Yang, X. Wang, Q. Fang, H. Dai, Y. Cao, X. Wei, An online soc and capacity estimation method for aged lithium-ion battery pack considering cell inconsistency, Journal of Energy Storage 29 (2020) 101250.

[12] L. Ma, C. Hu, F. Cheng, State of charge and state of energy estimation for lithium-ion batteries based on a long short-term memory neural network, Journal of Energy Storage 37 (2021) 102440.

[13] H. Yang, X. Sun, Y. An, X. Zhang, T. Wei, Y. Ma, Online parameters identification and state of charge estimation for lithium-ion capacitor based on improved cubature kalman filter, Journal of Energy Storage 24 (2019) 100810.

[14] H. F. Khan, A. Hanif, M. U. Ali, A. Zafar, A lagrange multiplier and sigma point kalman filter based fused methodology for online state of charge estimation of lithium-ion batteries, Journal of Energy Storage 41 (2021) 102843.

[15] L. Li, Y. Ren, K. O'Regan, U. R. Koleti, E. Kendrick, W. D. Widanage, J. Marco, Lithium-ion battery cathode and anode potential observer based on reduced-order electrochemical single particle model, Journal of Energy Storage 44 (2021) 103324.

[16] L. Ren, G. Zhu, J. Kang, J. V. Wang, B. Luo, C. Chen, K. Xiang, An algorithm for state of charge estimation based on a single-particle model, Journal of Energy Storage 39 (2021) 102644.

[17] H. Arunachalam, S. Onori, What if the doyle-fuller-newman model fails? a new macroscale modeling framework, in: 2018 IEEE Conference on Decision and Control (CDC), IEEE, 2018, pp. 5702–5707.

[18] H. Arunachalam, S. Onori, Full homogenized macroscale model and pseudo-2-dimensional model for lithium-ion battery dynamics: Comparative analysis, experimental verification and sensitivity analysis, Journal of The Electrochemical Society 166 (8) (2019) A1380–A1392.

[19] H. Arunachalam, S. Korneev, I. Battiato, S. Onori, Multiscale modeling approach to determine effective lithium-ion transport properties, in: 2017 American Control Conference (ACC), IEEE, 2017, pp. 92–97.

[20] H. Arunachalam, A new multiscale modeling framework for lithium-ion battery dynamics: Theory, experiments, and comparative study with the doyle-fuller-newman model, Ph.D. thesis, Clemson University (2017).

[21] N. A. Chaturvedi, R. Klein, J. Christensen, J. Ahmed, A. Kojic, Algorithms for advanced battery-management systems, IEEE Control systems magazine 30 (3) (2010) 49–68.

[22] H. Arunachalam, S. Onori, Full homogenized macroscale model and pseudo-2-dimensional model for lithium-ion battery dynamics: Comparative analysis, experimental verification and sensitivity analysis, Journal of The Electrochemical Society 166 (8) (2019) A1380–A1392.

[23] V. R. Subramanian, V. D. Diwakar, D. Tapriyal, Efficient macro-micro scale coupled modeling of batteries, Journal of The Electrochemical Society 152 (10) (2005) A2002–A2008.

[24] X. Han, M. Ouyang, L. Lu, J. Li, Simplification of physics-based electrochemical model for lithium ion battery on electric vehicle. part ii: Pseudo-two-dimensional model simplification and state of charge estimation, Journal of Power Sources 278 (2015) 814–825.

[25] Z. Deng, L. Yang, H. Deng, Y. Cai, D. Li, Polynomial approximation pseudo-two-dimensional battery model for online application in embedded battery management system, Energy 142 (2018) 838–850.

[26] F. A. Ortiz-Ricardez, A. Romero-Becerril, L. Alvarez-Icaza, Hard limitations of polynomial approximations for reduced-order models of lithium-ion cells, Journal of Applied Electrochemistry 50 (3) (2020) 343–354.

[27] Z. Deng, L. Yang, H. Deng, Y. Cai, D. Li, Polynomial approximation pseudo-two-dimensional battery model for online application in embedded battery management system, Energy 142 (2018) 838–850.

[28] T. R. Tanim, C. D. Rahn, C.-Y. Wang, State of charge estimation of a lithium ion cell based on a temperature dependent and electrolyte enhanced single particle model, Energy 80 (2015) 731–739.

[29] S. J. Moura, F. B. Argomedo, R. Klein, A. Mirtabatabaei, M. Krstic, Battery state estimation for a single particle model with electrolyte dynamics, IEEE Transactions on Control Systems Technology 25 (2) (2016) 453–468.

[30] L. O. Valøen, J. N. Reimers, Transport properties of lipf6-based li-ion battery electrolytes, Journal of The Electrochemical Society 152 (5) (2005) A882–A891.

Appendix A. Parameter Values

Temperature dependence plot of diffusion parameters and reaction rate parameter are obtained from [22].

Table A.9: Li-ion cell parameter values taken from[17],[18]

Name	Symbol	value
Capacity	Q	$1.9Ah$
Universal gas constant	R	$8.314J.K^{-1}.mol^{-1}$
Current collector resistance	R_c	0.027Ω
Electrolyte concentration	$C_{e,a}$	$10^3 mol.m^{-3}$
P2D Electrolyte conductivity	K_e	$0.048\Omega m^{-1}$
P2D Electrolyte diffusion constant	D_e	$0.99\times10^{-11}m^2.s^{-1}$
FHM Electrolyte conductivity	K_e	$0.06\Omega m^{-1}$
FHM Electrolyte diffusion constant	D_e	$1.18\times10^{-11}m^2.s^{-1}$

Table A.10: Li-ion electrode parameter values taken from [17],[18]

Name	Symbol	Anode	Cathode	Unit
Thickness	L	53.2	39.9	μm
Particle Radius	R_s	1.2	1.2	μm
Volume Fraction	η	0.626	0.574	-
Conductivity	K_e	113	113	$Amol^{-1}$
Max Concentration	$C_{j,m}$	27088	48700	$mol.m^{-3}$
Stoichiometry	θ	0.7916	0.3494	
Specific Inter-facial surface Area	a_s	15×10^5	15×10^5	